

22. T. A. Jones, J.-Y. Zou, S. W. Cowan, *Acta Crystallogr.* **A47**, 110 (1991).
23. A. T. Brünger, *J. Mol. Biol.* **203**, 803 (1988).
24. J. M. Moore, W. J. Chazin, R. Pows, P. E. Wright, *Biochemistry* **27**, 7806 (1988).
25. P. J. Kraulis, *J. Appl. Crystallogr.* **24**, 946 (1991).
26. D. J. Bacon and W. F. Anderson, *J. Mol. Graphics* **6**, 219 (1988).
27. E. A. Merritt and M. E. P. Murphy, *Acta Crystallogr.* **D50**, 869 (1994).
28. A. Nicholls, K. A. Sharp, B. Honig, *Proteins Struct. Funct. Genet.* **11**, 282 (1991).
29. C. E. Stebbins *et al.*, *Nature* **373**, 636 (1995).
30. Single-letter abbreviations for the amino acid residues are as follows: A, Ala; C, Cys; D, Asp; E, Glu; F, Phe; G, Gly; H, His; I, Ile; K, Lys; L, Leu; M, Met; N, Asn; P, Pro; Q, Gln; R, Arg; S, Ser; T, Thr; V, Val; W, Trp; and Y, Tyr.
31. We thank G. C. Ireton, E. Pohl, S. Turley, B. Bern-

stein, C. Verlinde, F. Athappilly, F. van den Akker, D. Chudzik, J. Yeh, and R. Li for their technical assistance and many engaging conversations; and Y. Pocker for helpful comments concerning the catalytic mechanism; H. Bellamy and P. Kuhn at the Stanford Synchrotron Radiation Laboratory for help with MAD and isomorphous data collection; and the staffs of Brookhaven National Laboratory, the Cornell High Energy Synchrotron Source, and the European Synchrotron Radiation Facility for their support with data collection. This work was supported by grant GM49156 from NIH (to J.J.C.), by American Cancer Society grant PF-3905 (to L.S.), by an NIH fellowship grant GM16713 to X.Q., and by a major equipment grant from the Murdock Charitable Trust to the Biomolecular Structure Center and grant CA65656 from NIH (to W.G.J.H.).

1 December 1997; accepted 28 January 1998

Natural Ligand of Mouse CD1d1: Cellular Glycosylphosphatidylinositol

Sebastian Joyce,* Amina S. Woods, Jonathan W. Yewdell,
Jack R. Bennink, A. Dharshan De Silva, Alina Boesteanu,
Steven P. Balk, Robert J. Cotter, Randy R. Brutkiewicz

Mouse CD1d1, a member of the CD1 family of evolutionarily conserved major histocompatibility antigen-like molecules, controls the differentiation and function of a T lymphocyte subset, NK1⁺ natural T cells, proposed to regulate immune responses. The CD1d1 crystal structure revealed a large hydrophobic binding site occupied by a ligand of unknown chemical nature. Mass spectrometry and metabolic radiolabeling were used to identify cellular glycosylphosphatidylinositol as a major natural ligand of CD1d1. CD1d1 bound glycosylphosphatidylinositol through its phosphatidylinositol aspect with high affinity. Glycosylphosphatidylinositol or another glycolipid could be a candidate natural ligand for CD1d1-restricted T cells.

The CD1 region encodes a family of evolutionarily conserved proteins that closely resemble the classical antigen presenting major histocompatibility complex (MHC) molecules (1, 2). CD1d controls the function of NK1⁺ natural T (NKT) cells (3, 4), an unusual subset of T lymphocytes that express receptors for natural killer cells (NKRP-1C) and T cells [$\alpha\beta$ or $\gamma\delta$ T cell receptor (TCR)] (5). NKT cells are thought to play an immunoregulatory role in responses to foreign and self antigens (6, 7).

Maturation of NKT cells depends on the interaction of the TCR with CD1d1 (8–10). It is unclear whether this interaction requires the display of specific ligands in the CD1d1 groove akin to those presented by MHC molecules. Because the TCR repertoire of NKT cells is highly restricted (11–13), they probably interact with ligand-free CD1d1 or with CD1d1 displaying a highly conserved ligand. The three-dimensional structure of CD1d1 revealed a large hydrophobic binding site occupied by ligands whose chemical nature could not be determined with the diffraction data (2).

Natural ligands of CD1d1 were isolated from purified CD1d1 molecules expressed by TAP (transporters associated with antigen processing)-deficient human T2 cells infected with a recombinant vaccinia virus expressing the CD1d1 gene (3, 14). Low molecular weight ligands associated with CD1d1 and HLA class I molecules (the latter serving as controls) were isolated and fractionated by reversed-phase high-performance liquid chromatography (RP-HPLC) as described (15, 16). Several peaks were observed at 210 nm (detects peptide and

double bonds) that were associated only with CD1d1-derived material (Fig. 1A). Very little, if any, absorbance was detected at 254 or 280 nm (detects aromatic amino acids) (17). The major peak present in CD1d1-derived material (Fig. 1A, arrow) corresponds to a minor peak in the fractions from HLA-associated ligands. Each of the six fractions constituting the major peak (about 82 and 85 min) were refractionated by RP-HPLC with a mixture of C₁₈ and cation-exchange (1:1) matrix (18). This yielded single peaks that behaved in an indistinguishable manner (17). Similar refractionation of the HLA class I-associated material eluting between about 82 and 85 min did not yield any signal (17), probably because the chemical constitution of this material prevented its recovery.

Thus, the major peak eluting between about 82 and 85 min represents a CD1d1 ligand. To identify this material, we subjected it to matrix-assisted laser-desorption/ionization mass spectrometric (MALDI-MS) analysis (19). The positive ion mass spectra of each of the six refractionated fractions contained peaks at m/z 598, 614, 636, 1211, and 1227 (Fig. 1B), conclusively showing their identity to one another. MALDI-MS analysis after digestion of these samples with either carboxypeptidase or aminopeptidase indicated that the ligands associated with CD1d1 were not peptidic (17).

The CD1d1-associated natural ligand was incubated with ammonium sulfate (19) to enhance the ion signal in the mass spectrometer (20). This resulted in the loss of signals at m/z 1211 and 1227 and the gain of signal at m/z 887 (Fig. 1C). The peak at m/z 887 was consistent with the mass of a protonated molecular ion (MH⁺) of a phospholipid (21). The negative ion mass spectrum (19) of the sample treated with ammonium sulfate revealed a (MH)⁻ ion of the same species at m/z 885.3 and a fragment ion at m/z 705.6 (Fig. 1D) resulting from the characteristic, and nearly diagnostic, loss of an inositol head group (22).

From these three mass spectra, one solution to the identity of the peak at m/z 1211 is that it is the MH⁺ ion for a phosphatidylinositol-diglycoside containing stearic and arachidonic acids, glucosamine, and mannose, with a calculated mass of 1211.4 daltons. Because it contains a negatively charged phosphate group, it is unstable and hence of relatively low intensity in the positive ion mass spectrum (Fig. 1B). Under high laser power it decomposes, cleaving the C²-C³ bond of glycerol to form a stable fragment ion at m/z 614 that lacks a phosphate. The m/z 614 ion was the most abundant ion in the mass spectrum and was used to determine the identities of the acyl

S. Joyce, A. D. De Silva, A. Boesteanu, Department of Microbiology and Immunology, The Pennsylvania State University College of Medicine, Milton S. Hershey Medical Center, Hershey, PA 17033-0850, USA.

A. S. Woods and R. J. Cotter, Departments of Oncology and Pharmacology and Molecular Sciences, The Johns Hopkins University School of Medicine, Baltimore, MD 21205-2185, USA.

J. W. Yewdell, J. R. Bennink, R. R. Brutkiewicz, Laboratory of Viral Diseases, National Institute of Allergy and Infectious Diseases, National Institutes of Health, Bethesda, MD 20892-0440, USA.

S. P. Balk, Hematology-Oncology Division, Beth Israel Deaconess Medical Center, Harvard Medical School, Boston, MA 02215, USA.

*To whom correspondence should be addressed. E-mail: sjoyce@bcmic.hmc.psu.edu

groups as stearic acid and arachidonic acid. The peak at m/z 1227, 16 mass units greater than the peak at m/z 1211 (Fig. 1B), was a related structure that appears to result from the decomposition of larger glycosylphosphatidylinositol (GPI) structures. Treatment of the sample material with ammonium sulfate (Fig. 1, C and D) may have resulted in hydrolysis of the diglycoside linked to inositol, leading to the observation of the MH^+ and $(MH)^-$ ions of phosphatidylinositol (PI) in these two mass spectra, respectively. Thus, the material recovered from CD1d1 is probably GPI.

The biological significance of GPI association with CD1d1 was potentially undermined by the conditions of its isolation; namely, the use of detergent to solubilize CD1d1, vaccinia virus to express CD1d1, or the monoclonal antibodies (mAbs) used for HLA depletion and CD1d1 recovery. Therefore we repeated this analysis with CD1d1 molecules purified in a completely different manner. Soluble CD1d1 (sCD1d1), tagged with His⁶ at its carboxyl terminus, secreted by engineered mouse cells was purified by Ni-affinity chromatography (23). Several peaks at 210 nm were associated only with the ligands isolated from sCD1d1 [HPLC conditions were different from those used in the experiment in Fig. 1 (16, 18, 23), which accounts for the

different profile] but not from soluble H-2D^b (Db-sol) (Fig. 2A). MALDI-MS analysis of these peaks revealed ions with m/z identical to that observed with the ligand eluted from CD1d1 expressed by T2 cells (Fig. 2B) (17) as well as additional ions arising from larger GPI structures (Fig. 2B). Similar larger ion species, $m/z > 1227$, observed in Fig. 2B were also observed in the ion spectra described in Fig. 1 but were of lower intensity (17), probably owing to their loss or decomposition during multiple RP-HPLC. Additionally, the smaller ion species, $m/z < 886$, were also observed in the ion spectrum shown in Fig. 2B but were of very low intensity (17). Thus, the recovery of material from CD1d1, tentatively identified as GPI by MALDI-MS, occurs under different conditions of CD1d1 expression and purification and is a bona fide ligand for CD1d1 in cells. The identified natural CD1d1-associated ligand resembled the mammalian GPI moiety of the glycolipid-anchored proteins (24).

To independently confirm that CD1d1 binds GPI, cells expressing sCD1d1 and control cells expressing Db-sol were metabolically labeled with components of GPI: [³H]arachidonic acid, [³H]mannose, or [³H]ethanolamine (25). Each of the radiolabels was recovered with purified CD1d1

but not with Db-sol (Fig. 3A). Because [³H]mannose can also be incorporated into the carbohydrate modification of sCD1d1 heavy chain, the ligand associated with [³H]mannose-labeled sCD1d1 and Db-sol were separated from the heavy and light chains by Microcon-10 filtration (25). [³H]Mannose label was recovered only from sCD1d1 and not from Db-sol, which collected into the filtrate (Fig. 3A, insets), showing that mannose is incorporated into GPI.

Based on the hydrophobic nature of the CD1d1 ligand binding site (2), GPI would be predicted to bind CD1d1 through its PI group. This was tested in an *in vitro* binding assay (26), which revealed that [³H]PI specifically bound sCD1d1 but not H-2D^b (Fig. 3B). Binding of [³H]PI to sCD1d1 occurred in the micromolar range (17) with a dissociation constant of $\sim 0.4 \mu M$ calculated by Scatchard analysis (Fig. 3C).

Thus, GPI is a major detectable ligand of CD1d1, representing >90% of the low molecular weight material recovered (27). Peptides were previously identified as CD1d1 ligands (28). These peptides are highly hydrophobic, contain numerous aromatic residues (28), and would therefore be detected by absorption at 254 or 280 nm. Our recovery of extremely small amounts of CD1d1 ligands that absorb at 254 and 280 nm

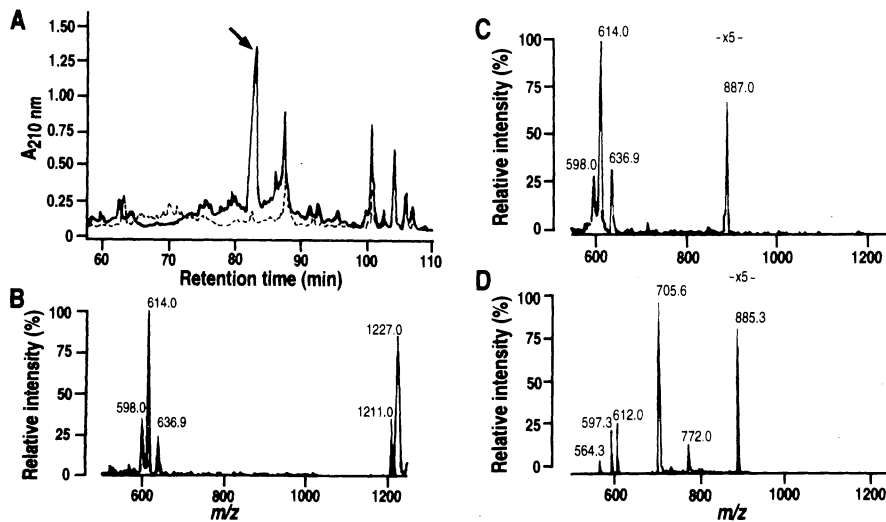


Fig. 1. CD1d1 binds glycosylated PI. (A) RP-HPLC profile at A_{210} of CD1d1 (solid line) and control endogenous HLA class I (broken line)-associated ligands isolated as described (16). An aliquot of each fraction eluting between 58 and 95 min of CD1d1 and HLA-associated ligands was analyzed by MALDI-MS. A complex array of ion spectra was observed for both samples (17). (B) MALDI-MS analysis of each of the fractions constituting a refracted peak (16, 18) of the CD1d1-associated ligand showing a representative positive ion mode mass spectrum of the ligand that contains ions at m/z 614, 1211, and 1227. (C) A positive ion mass spectrum upon adding saturated ammonium sulfate results in a new peak at m/z 887 and the loss of ions at m/z 1211 and 1227. (D) The negative ion mode spectrum of sample in (C) in the presence of saturated ammonium sulfate. The peak at m/z 885.3 is the $(MH)^-$ ion of the species observed at m/z 886 in the positive ion mode. An additional peak is observed at m/z 705.6 that corresponds to the loss of a hexose, presumably inositol. Note that different fragments derived from the same molecule form stable positive (C) and negative (D) ions. Together the positive and negative ion spectra provide complementary structural information.

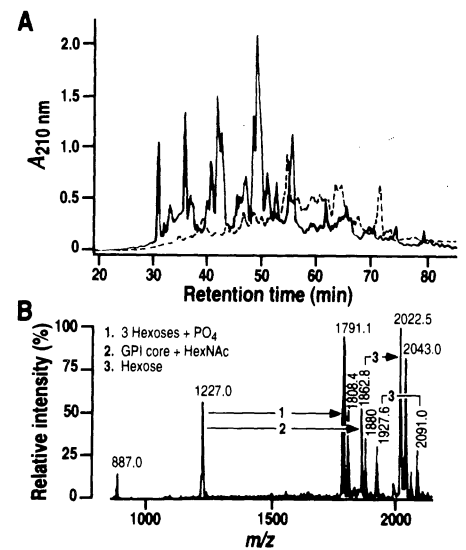


Fig. 2. GPI is the natural ligand of CD1d1. (A) RP-HPLC profile at A_{210} of the sCD1d1 (solid line) and control Db-sol (broken line)-associated ligands eluted on a different gradient than that used in Fig. 1A (16, 18, 23). (B) A representative positive ion mass spectrum of the sCD1d1-associated natural ligand. All sCD1d1-associated peaks analyzed showed similar ion spectra. In addition to the ions at m/z 887 and 1227, several new ion peaks were observed at m/z 1791.2, 1862.8, and 2022.5; the ion at m/z 2043 could be the MNa^+ salt of the dominant ion at m/z 2022.5.

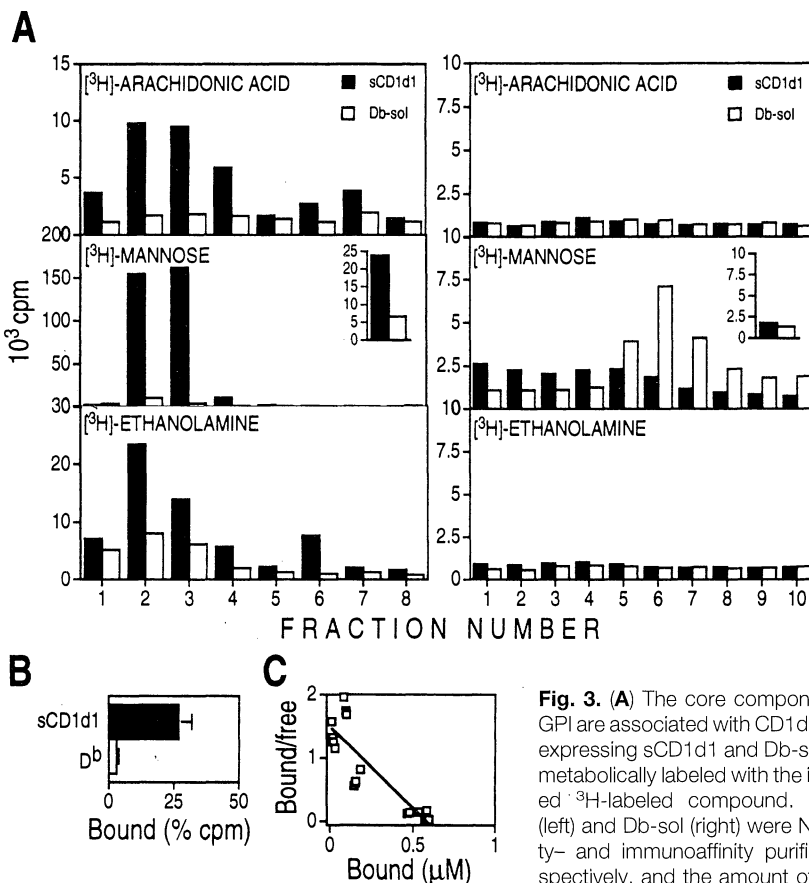


Fig. 3. (A) The core components of GPI are associated with CD1d1. Cells expressing sCD1d1 and Db-sol were metabolically labeled with the indicated ^3H -labeled compound. CD1d1 (left) and Db-sol (right) were Ni-affinity- and immunoaffinity purified, respectively, and the amount of radioactivity incorporated was monitored

by scintillation counting (25). The background was derived from Db-sol supernatant (left) and sCD1d1 supernatant (right) that nonspecifically bound to Ni-Sepharose and B22-249-coupled protein A-Sepharose, respectively. sCD1d1 elutes into fractions 2 and 3 and Db-sol elutes into fractions 5, 6, and 7. ^3H Mannose-labeled ligand was separated from sCD1d1 and Db-sol by Microcon-10 filtration. The label was recovered from the filtrate of only CD1d1-associated material (insets). Thus, the label was incorporated into GPI. **(B)** CD1d1 specifically binds GPI through its PI aspect but does not bind H-2D^p, a classical antigen presenting class I molecule, or immunoglobulins (17). **(C)** Scatchard analysis of ^3H PI binding to sCD1d1 (26) revealed a dissociation constant of $\sim 0.4 \mu\text{M}$.

suggests that similar cellular peptides are not major natural ligands for CD1d1. The ubiquitous occurrence of GPI in different cell types is consistent with the pattern of NKT cell recognition of CD1d1 molecules. Alternatively, GPI may provide a chaperone function by occupying the groove of nascent CD1d1 molecules, preserving the folded conformation until an alternative self or a foreign glycolipid is loaded in a distal secretory compartment. Because GPI is present in the lumen of the endoplasmic reticulum (ER), where it is added to the carboxyl terminus of glycolipid-anchored proteins (29), GPI binding to CD1d1 molecules could occur there. This is consistent with the finding that sCD1d1 also naturally associates with GPI. CD1d1 molecules, like other CD1 family members, possess a motif in their cytosolic tails that direct them to endosomes (30), presumably for the loading of exogenous antigens. In this case, ER-loaded GPI would have to be removed to allow for association with the exogenous

ligand. A specific mechanism may be required for this process, akin to the removal of invariant chain-derived CLIP peptide (MHC class II-associated invariant chain-derived peptide) from newly assembled MHC class II molecules by H2-M or HLA-DM glycoproteins (31).

REFERENCES AND NOTES

1. L. H. Martin, F. Calabi, C. Milstein, *Proc. Natl. Acad. Sci. U.S.A.* **83**, 9154 (1986).
2. Z.-H. Zeng *et al.*, *Science* **277**, 339 (1997).
3. A. Bendelac *et al.*, *ibid.* **268**, 863 (1995).
4. M. Exley, G. Garcia, S. P. Balk, S. Porcelli, *J. Exp. Med.* **186**, 109 (1997).
5. M. Sykes, *J. Immunol.* **145**, 3209 (1990).
6. T. Yoshimoto, A. Bendelac, C. Watson, J. Hu-Li, W. E. Paul, *Science* **270**, 1845 (1995).
7. A. G. Baxter, S. J. Kinder, K. J. L. Hammond, R. Scollay, D. I. Godfrey, *Diabetes* **46**, 572 (1997).
8. S. T. Smiley, M. H. Kaplan, M. J. Grusby, *Science* **275**, 977 (1997).
9. Y.-H. Chen, N. M. Chiu, M. Mandal, N. Wang, C.-R. Wang, *Immunity* **6**, 459 (1997).
10. S. K. Mendiratta *et al.*, *ibid.*, p. 469.
11. H. Arase, N. Arase, K. Agasawara, R. A. Good, K. Onoe, *Proc. Natl. Acad. Sci. U.S.A.* **89**, 6506 (1992).

12. E. G. Brooks *et al.*, *ibid.* **90**, 11787 (1993).
13. O. Lantz and A. Bendelac, *J. Exp. Med.* **180**, 1097 (1994).
14. R. R. Brutkiewicz, J. R. Bennink, J. W. Yewdell, A. Bendelac, *ibid.* **182**, 1913 (1995).
15. S. Joyce, P. Tabaczewski, R. H. Angeletti, S. G. Nathanson, I. Stroynowski, *ibid.* **179**, 577 (1994).
16. Lacking a suitable CD1-specific antibody or antiserum, we exploited the observation that the NKT cell-activation function of CD1d1 is TAP independent and β_2 -microglobulin ($\beta_2\text{m}$) dependent (14). CD1d1 was affinity purified with a mAb to human $\beta_2\text{m}$ from TAP-deficient human T2 cells infected with a recombinant vaccinia virus (VV) expressing the CD1d1 cDNA (3, 14). The T2 cells are not completely devoid of endogenous class I molecules bearing low molecular weight ligands (32); these were first removed from detergent extracts by using a mixture of mAbs to HLA-A, -B, and -C. About 10^{10} T2 cells infected with VV-CD1d1 at a multiplicity of infection of ~ 3 for 4 to 5 hours were detergent solubilized, and HLA class I was isolated by using protein A-Sepharose (Repligen) coupled with a mixture of specific mAbs (HB95, HB116, HB118, and HB120; a kind gift from T. Mohanakumar) followed by the purification of CD1d1 by using a specific mAb to human $\beta_2\text{m}$ (HB28; ATCC). HLA class I and CD1d1-associated ligands were isolated, separated, and fractionated by RP-HPLC as described (15). Briefly, sample was injected in buffer A [0.06% trifluoroacetic acid (TFA) in water] onto a reversed-phase C_{18} column (1.0×250 mm; Alltech) and eluted immediately by using a buffer B (0.05% TFA containing acetonitrile) gradient starting at 0% at 10 min to 37, 70, 90, and 100% at 73, 105, 115 and 120 min, respectively, at $50 \mu\text{l}/\text{min}$.
17. S. Joyce *et al.*, unpublished data.
18. Second-dimension RP-HPLC was performed with a 1:1 mixture of C_{18} and cation-exchange column (1.0×250 mm; Alltech) by achieving 15, 60, and 100% buffer B at 15, 105, and 125 min, respectively, at $50 \mu\text{l}/\text{min}$.
19. Mass spectra were acquired on a Kratos analytical MALDI-4 mass spectrometer equipped with a curved-field reflectron and a nitrogen laser. About 0.3 to $1.0 \mu\text{l}$ of each fraction (30 to 40 μl), either directly or after concentrating to $\sim 15 \mu\text{l}$, was applied onto the sample probe. Matrix, saturated α -cyano-4-hydroxycinnamic acid in 45% ethanol containing 8.8% formic acid (~ 300 nl), was then applied to the sample. A replicate of the sample was similarly spotted, except that, to enhance ion signal, 300 nl of saturated ammonium sulfate was added before matrix (20). Spectra were acquired in positive and negative modes as well as in linear and reflectron modes after application of a 20-kV accelerating voltage. Because different fragments form stable positive and negative ions, when derived from the same molecule, positive and negative spectra provide complementary structural information. The mass analyses reported here are within a mass accuracy of 0.5 dalton.
20. A. S. Woods *et al.*, *Anal. Biochem.* **226**, 15 (1995).
21. N. Heller, R. J. Cotter, C. Fenselau, O. M. Uy, *Anal. Chem.* **59**, 2806 (1987).
22. N. Heller, C. Murphy, R. J. Cotter, C. Fenselau, O. M. Uy, *ibid.* **60**, 2787 (1988).
23. Spent tissue culture supernatant containing sCD1d1 (~ 2 liters; to be described elsewhere) and Db-sol (~ 10 liters; to be described elsewhere) were concentrated by tangential flow filtration (Pall Filtron). CD1d1 was Ni-NTA-affinity purified (Qiagen's method) and Db-sol was immunoaffinity purified with B22-249, a H-2D^p-specific mAb-coupled protein A-Sepharose (Repligen). Low molecular weight ligands were isolated from ~ 3.0 mg of sCD1d1 and Db-sol and fractionated by C_{18} RP-HPLC. Sample elution was initiated after the injection front returned to zero by increasing buffer B concentration to 37, 70, 90, and 100% at 63, 95, 105, and 110 min, respectively, at $50 \mu\text{l}/\text{min}$.
24. A. W. Homans *et al.*, *Nature* **333**, 269 (1988).
25. About 3 to 5×10^7 sCD1d1 and Db-sol cells were labeled with $62.5 \mu\text{Ci}$ of $[5,6,8,9,11,12,14,15\text{-}^3\text{H}]\text{arachidonic acid}$, $250 \mu\text{Ci}$ of $[1\text{-}^3\text{H}]\text{ethanolamine-HCl}$, or $250 \mu\text{Ci}$ of $\text{D-}[2\text{-}^3\text{H}]\text{mannose}$ (American Ra-

diolabeled Chemicals). [³H]Mannose labeling was done in glucose-free and L-glutamine-free medium supplemented with 5% dialyzed fetal bovine serum, dextrose (0.5 mg/ml), sodium pyruvate (1.1 mg/ml), antibiotics, nucleosides, and nonessential amino acids for 18 to 24 hours at 37°C. CD1d1 and Db-sol in the culture supernatant were purified with His-Trap Ni-Sepharose and B22-249-coupled protein A-Sepharose columns, respectively, after preclearing with Hi-Trap protein A-Sepharose according to the manufacturer (Pharmacia Biotech). Radioactivity in each fraction was monitored with a scintillation counter (Beckman). [³H]Mannose-labeled, sCD1d1 and Db-sol-associated ligands were separated from the heavy and light chains by Microcon-10 (Amicon) filtration to specifically monitor GPI-associated radioactivity.

26. sCD1d1 and H-2D^b (about 4 μM), in triplicate, were mixed with 1.8 μCi of L-α-[myo]-inositol-2-³H]PI (11 Ci/mmol; DuPont-NEN) in 100 μl of phosphate-buffered saline at 37°C for about 18 hours. sCD1d1- and H-2D^b-bound [³H]PI were separated from free [³H]PI by Microcon-10 filtration, and radioactivity in the retained solution was measured in a scintillation counter. H-2D^b reconstituted in vitro from heavy and

light chains produced in *Escherichia coli* and with a H-2D^b-binding peptide, Gly-Ala-Ile-Ser-Asn-Met-Tyr-Ala-Met, derived from glutamic acid dehydrogenase was used as the control for binding specificity. The in vitro reconstituted H-2D^b was generously provided by E. Palmieri and S. G. Nathenson. For Scatchard analysis, various concentrations of purified sCD1d1, in duplicate, were mixed with 1.8 μCi of [³H]PI (~1.6 μM) in 100 μl of 20 mM phosphate buffer, pH 7.4. After incubation at 37°C for ~18 hours, sCD1d1-[³H]PI complexes were separated from free [³H]PI by Microcon-10 filtration, and radioactivity in the retained solution was measured.

27. Clearly GPI is the major ligand identified under the conditions described here for the isolation, RP-HPLC fractionation, and MALDI-MS analysis (Fig. 1). To determine whether GPI is the major or the only natural ligand of CD1d1, we estimated the percent of CD1d1 occupied by GPI from the ratio of [³H]mannose-labeled heavy chain to [³H]mannose-labeled GPI. Considering that D-[2-³H]mannose converts mostly to D-[2-³H]fucose and rarely to other sugars (33), there are about seven times as many mannoses and fucoses in the heavy chain as in GPI (17). Thus ~65% of CD1d1 is occupied by GPI before account-

ing for losses incurred during the purification steps. Assuming 65 to 70% recovery of the ligand [based on peptide recoveries from class I molecules (15, 34)], then >90% of CD1d1 is occupied by GPI.

28. A. R. Castaño *et al.*, *Science* **269**, 223 (1995).
29. S. Udenfriend and K. Kodukula, *Annu. Rev. Biochem.* **64**, 563 (1995).
30. M. Sugita *et al.*, *Science* **273**, 349 (1996).
31. P. R. Wolfe and H. L. Ploegh, *Annu. Rev. Cell Biol.* **11**, 267 (1995).
32. R. A. Henderson *et al.*, *Science* **255**, 1264 (1992).
33. A. Varki, *Methods Enzymol.* **230**, 16 (1994).
34. T. S. Jardetzky, W. S. Lane, R. A. Robinson, D. R. Madden, D. C. Wiley, *Nature* **353**, 326 (1991).
35. We thank M. H. Hunsinger and J. M. Weaver for technical assistance; T. Mohanakumar, E. Palmieri, and S. G. Nathenson for generously providing affinity-purified anti-HLA class I mAb and reconstituted H-2D^b, respectively; and A. K. Menon for helpful discussions. Supported by grants from NIH (S.J., S.P.B., and R.J.C.), the Juvenile Diabetes Foundation International (S.J.), the American Cancer Society (S.J.), and the National Research Council-NIH (R.R.B.).

16 September 1997; accepted 16 January 1998

A Screen for Genes Induced in the Suprachiasmatic Nucleus by Light

Mary E. Morris, N. Viswanathan, Sandra Kuhlman, Fred C. Davis, Charles J. Weitz*

The mechanism by which mammalian circadian clocks are entrained to light-dark cycles is unknown. The clock that drives behavioral rhythms is located in the suprachiasmatic nucleus (SCN) of the brain, and entrainment is thought to require induction of genes in the SCN by light. A complementary DNA subtraction method based on genomic representational difference analysis was developed to identify such genes without making assumptions about their nature. Four clones corresponded to genes induced specifically in the SCN by light, all of which showed gating of induction by the circadian clock. Among these genes are *c-fos* and *nur77*, two of the five early-response genes known to be induced in the SCN by light, and *egr-3*, a zinc finger transcription factor not previously identified in the SCN. In contrast to known examples, *egr-3* induction by light is restricted to the ventral SCN, a structure implicated in entrainment.

Daily rhythms of biological activity, manifested by forms as diverse as cyanobacteria, fungi, plants, and animals, are driven by self-sustaining, endogenous oscillators called circadian clocks (1), which typically run with an intrinsic period that is close to, but not exactly, 24 hours. Under natural conditions, circadian clocks become precisely entrained to the 24-hour light-dark cycle because exposure to light at certain times induces a phase shift of the clock. Entrainment to light-dark cycles ensures that the clock adopts a specific and stable phase relation to the natural day, setting the clock to local time and enabling the organism to anticipate daily environmental events (2).

In mammals, the circadian clock that drives daily rhythms of behavioral activity is located within the SCN of the hypothalamus (3). Entrainment of the clock to light-dark cycles is mediated by photoreceptors in the retina (4), and light information is conveyed directly from the retina to the SCN by the retinohypothalamic tract (5). Although the molecular basis of entrainment to light-dark cycles in mammals is unknown, the process likely involves light- and clock-dependent transcriptional regulation within the SCN (6). When a rodent kept in constant darkness is exposed to a brief light pulse during the subjective night, a time when the clock responds to light with a phase shift, five known early-response genes—*c-fos*, *fos-B*, *jun-B*, *zif268* (NGFI-A), and *nur77* (NGFI-B)—are specifically induced within the SCN (7). The genes are not induced by exposure to light during the subjective day, a time when the clock is not phase-shifted by light. Togeth-

er, these and related experiments (8) strongly suggest that induction of genes in the SCN by light is an intermediate step in a pathway mediating entrainment of the clock to light-dark cycles. They further suggest that gating of this induction by the clock contributes to the restriction of phase-shifting by light to certain times, a feature that is essential for achieving stable entrainment (9).

To discover potential components of the entrainment pathway, we sought to identify genes induced in the SCN by light without making assumptions about their nature. We developed a cDNA subtraction method based on genomic representational difference analysis (RDA) (10) and carried out subtractions as follows: Syrian hamsters were entrained to a light-dark cycle for 3 weeks and then placed in constant dim light (<1 lux) for 1 week (11). Animals were then assigned to either of two equal groups for light treatment (30 min, 250 lux) or sham treatment (similar handling, <1 lux) at circadian time (CT) 19, a time during subjective night that is optimal for a phase advance by light. At the end of the treatment, SCNs were removed by micropunch from 40 animals in each group. The remaining animals served as controls (Fig. 1). As expected, light treatment resulted in a phase advance (Fig. 1A), whereas sham treatment resulted in little or no phase shift (Fig. 1B).

Starting with 1 μg of polyadenylated RNA from each of the two groups of 40 SCN tissue punches, we generated cDNA representations (12). Each RDA experiment (13) was performed so as to identify genes induced by light ("forward") and genes suppressed by light ("reverse") (13), the latter used here solely as a control. After three rounds of RDA, polymerase chain reaction (PCR) products were cloned and

M. E. Morris and C. J. Weitz, Department of Neurobiology, Harvard Medical School, Boston, MA 02115, USA. N. Viswanathan, S. Kuhlman, F. C. Davis, Department of Biology, Northeastern University, Boston, MA 02115, USA.

*To whom correspondence should be addressed.